AGU ADVANCING EARTH AND SPACE SCIENCE

Earth's Future

RESEARCH ARTICLE
10.1029/2020EF001825

Key Points:

- We have computed regional sea-level projections, consistent with regional climate projections from an ensemble of Earth System Models
- Regional climate processes impose correlations between sea-level components that cannot be derived from global mean surface temperature
- Correlations prescribed in the IPCC's fifth assessment report lead to overestimated projection uncertainties exceeding 100% regionally

Supporting Information:

- Supporting Information S1

Correspondence to:
E. Lambert,
erwin.lambert@knmi.nl

Citation:
Lambert, E., Le Bars, D., Goelzer, H., & van de Wal, R. S.W. (2021). Correlations between sea-level components are driven by regional climate change. *Earth's Future*, *9*, e2020EF001825. https://doi.org/10.1029/2020EF001825

Received 25 SEP 2020
Accepted 6 JAN 2021

Author Contributions:
Conceptualization: Dewi Le Bars, Heiko Goelzer, Roderik S.W. van de Wal
Data curation: Dewi Le Bars
Funding acquisition: Roderik S.W. van de Wal
Investigation: Dewi Le Bars, Heiko Goelzer, Roderik S.W. van de Wal
Methodology: Dewi Le Bars, Heiko Goelzer, Roderik S.W. van de Wal
Project Administration: Roderik S.W. van de Wal
Resources: Heiko Goelzer, Roderik S.W. van de Wal
Software: Dewi Le Bars

Correlations Between Sea-Level Components Are Driven by Regional Climate Change

Erwin Lambert[1,2], Dewi Le Bars[2], Heiko Goelzer[1,3,4], and Roderik S.W. van de Wal[1,5]

[1]Institute for Marine and Atmospheric Research Utrecht, Utrecht University, Utrecht, The Netherlands, [2]Meteorological Institute (KNMI), De Bilt, The Netherlands, [3]Laboratoire de Glaciologie, Université Libre de Bruxelles, Brussels, Belgium, [4]NORCE Norwegian Research Centre, Bjerknes Centre for Climate Research, Bergen, Norway, [5]Department of Physical Geography, Utrecht University, Utrecht, The Netherlands

Abstract The accurate quantification of uncertainties in regional sea-level projections is essential for guiding policy makers. As climate models do not currently simulate total sea level, these uncertainties must be quantified through summation of uncertainties in individual sea-level components. This summation depends on the correlation between the components, which has previously been prescribed or derived from each individual component's dependence on global mean surface temperature. In this study, we quantify, for the first time, regional correlations between sea-level components based on regional climate change projections. We compute regional sea-level projections consistent with climate projections from an ensemble of 14 Earth System Models. From the multi-model spread, we estimate the uncertainty in the regional climate's response to greenhouse forcing. To quantify the total uncertainty, we add the uncertainty in the response of sea-level components to this regional climate change. This approach reveals how regional climate processes impose correlations between sea-level components, affecting the total uncertainty. One example is an anti-correlation between North Atlantic sterodynamic change and Antarctic dynamic mass loss, suggesting a teleconnection established by the large-scale ocean circulation. We find that prescribed correlations, applied in the fifth assessment report of the Intergovernmental Panel on Climate Change, lead to a global overestimation in the uncertainty in regional sea-level projections on the order of 20%. Regionally, this overestimation exceeds 100%. We conclude that accurate uncertainty estimates of regional sea-level change must be based on projections of regional climate change and cannot be derived from global indicators such as global mean surface temperature.

Plain Language Summary Projections of future sea-level rise come with a great uncertainty. To inform policy makers, it is essential to accurately quantify the uncertainty in regional sea-level rise. This is difficult, as climate models do not simulate all processes that contribute to sea-level rise. In this study, we have developed a new method to quantify the uncertainty in regional sea-level rise, which is consistent with climate projections from a set of 14 climate models. We conclude that a number of processes in the climate system link together the different sea-level components. This interdependency affects the uncertainty in future projections. This interdependency was previously accounted for in the fifth assessment report of the Intergovernmental Panel on Climate Change. Here, we find that their method leads to an overestimation of uncertainties which are on the order of 20% globally. Regionally, uncertainties are overestimated by more than 100%. Altogether, we conclude that regional climate processes must be accounted for in order to accurately quantify the uncertainty in future sea-level projections.

1. Introduction

One of the most widespread and impactful consequences of climate change is sea-level rise (Oppenheimer et al., 2019). Facing this change, policy makers are challenged with mitigating and adapting to sea-level rise. The scientific information underlying policy decisions is commonly derived from probabilistic projections for a number of greenhouse gas emission scenarios (e.g., the Representative Concentration Pathways, or RCPs Vuuren et al., 2011). Such projections include an explicit quantification of the uncertainty. Probabilistic projections of sea-level rise have previously been used in decision making (e.g., Hall et al., 2019) and are the recommended type of scientific input for decision making for users with a medium to high uncertainty

Supervision: Roderik S.W. van de Wal
Validation: Heiko Goelzer, Roderik S.W. van de Wal
Writing – review & editing: Dewi Le Bars, Heiko Goelzer, Roderik S.W. van de Wal

tolerance (Hinkel et al., 2019). In addition, scenario-based probabilistic projections offer a useful benchmark to track the progress of scientific insight (e.g., Garner et al., 2018).

Probabilistic projections of climate change are most commonly based on ensemble simulations with Earth System Models (ESMs, e.g., Eyring et al., 2016). These numerical models describe a coupled atmosphere-ocean-land system and are used to simulate the consequences of, for example, increased greenhouse gas concentrations in the atmosphere. Probabilistic projections are then typically expressed in terms of the multi-model median projection as a central estimate and the multi-model spread as a measure for the associated uncertainty (e.g., Church et al., 2013). For sea-level rise, this ensemble-based method to quantify probabilistic projections cannot be directly applied, as ESMs do not simulate all components of sea-level rise. In particular ice mass loss from ice sheets, glaciers and ice caps, and changes in landwater storage, are not routinely simulated by ESMs. Instead, the climate output from ESMs is applied as external forcing to dedicated models, such as ice sheet models, to project the contributions of these components to future sea-level rise (e.g., Goelzer et al., 2020; Marzeion et al., 2020; Seroussi et al., 2020). This two-step approach complicates the quantification of probabilistic sea-level projections: in the summation of the uncertainties of individual components, assumptions must be made on the correlation between these components.

Formally, the correlation is a measure for the interdependency between two uncertain values. Consider the example of two sea-level components, say thermosteric expansion and glacier mass loss. Although these processes are unlikely to directly impact each other, both are strongly dependent on the amount of global warming. More warming will lead to both a greater thermosteric expansion of seawater and to a greater mass loss from glaciers. This shared dependency on global heat uptake implies a positive correlation between these two components. Assumptions on the correlation between all sea-level components influence the estimated uncertainty in total sea-level rise. According to the Special Report on Oceans and Cryosphere in a Changing Climate (SROCC, Oppenheimer et al., 2019) of the Intergovernmental Panel on Climate Change (IPCC), the uncertainty in the contributions of thermosteric expansion and glacier mass loss to global mean sea-level rise by the end of the century is ±4 and ±6 cm, respectively, under the mid-range emission scenario RCP 4.5. If these two components are independent of each other, the uncertainty in their sum would be ±7 cm, if they would be perfectly co-dependent (correlation 1), this would be ±10 cm. The difference between these uncertainties stems from the covariance between the components, which is a function of the correlation. This correlation is thus a crucial ingredient in the construction of probabilistic sea-level projections and can significantly impact high-end projections (Bamber et al., 2019), in particular when a comprehensive set of sea-level components is included (Le Bars, 2018).

The actual impact of sea-level rise is induced by changes in regional sea-level (RSL), rather than its global mean (Jevrejeva et al., 2019; Wal et al., 2019). Three methods have previously been applied to deal with correlations in projections of RSL. In order of increasing complexity, these are (1) assuming independence, (2) prescribing a mixture of independence and perfect codependence, and (3) deriving the correlation from the dependence on global mean surface temperature (GMST). The first method, where all sea-level components are assumed to be independent of each other, has been adopted in a number of studies (Jackson & Jevrejeva, 2016; Jevrejeva et al., 2016; Kopp et al., 2014). The second method was applied to the RSL projections in the IPCC's fifth assessment report (AR5, Church et al., 2013) and later also in SROCC. In this method, the sterodynamic and ice sheet surface mass balance (SMB) components are assumed to be perfectly co-dependent, whilst all other components (including glaciers and ice sheet dynamics) are assumed to be independent (Carson et al., 2015; Slangen et al., 2014). This quantification of regional uncertainties in sea-level projections deviates from the quantification of global uncertainties in AR5, for which a form of method 3 was developed. Using a Monte Carlo simulation, the uncertainty in GMST was propagated down to uncertainties in sea-level components. In this method, the correlations between sea-level components are thus derived from the GMST-dependence of each individual component. These implicit global correlations were reconstructed by Grinsted et al. (2015) to quantify the uncertainty in RSL projections. More recently, Palmer et al. (2020) enhanced the GMST-based approach of AR5 to apply the method consistently to both global and regional sea-level projections.

One may question whether GMST-dependence is an accurate precursor for the correlation between sea-level components. Global mean thermosteric expansion was found to be strongly influenced by the ocean heat uptake efficiency (Melet & Meyssignac, 2015). Glacier mass loss from Iceland, Greenland, and the Russian

Arctic is partially dependent on changes in ocean heat transport (Marzeion et al., 2012). Uncertainties in projected mass loss from the Greenland and Antarctic ice sheets are related to the simulation of present-day climate and future changes in regional atmospheric and oceanic temperature and precipitation (Barthel et al., 2020). For Greenland SMB specifically, Goelzer et al. (2020) attributed a significant uncertainty in projected mass loss to the uncertainty in warming over South West Greenland, while Fettweis et al. (2013) identified uncertainties in Arctic sea ice decline to impact changes in Northern Greenland SMB. These findings illustrate that it is not GMST that drives global and regional sea-level rise, but changes in regional climate. Because Earth's climate is a strongly coupled system, these regional changes in climate forcing may be co-dependent; and it is this co-dependence that imposes a correlation between sea-level components. An accurate assessment of this correlation should thus be based on changes in the complete climate system, rather than GMST alone.

In this study, we present a novel method to quantify the uncertainties in RSL projections. This method relies on the total climate change as simulated by an ensemble of ESMs, in order to quantify the correlation and covariance between components. The uncertainty in each sea-level component is separated into a *climate uncertainty*, based on the multi-model spread in climate forcing, and a *process uncertainty*, which measures the uncertain response to climate forcing for each component. This separation was recently illustrated for mass loss from the Greenland ice sheet (Goelzer et al., 2020) and glaciers (Marzeion et al., 2020). From the climate-uncertainty, we diagnose the correlation between components to identify the underlying physical mechanisms in the coupled climate system. Finally, we apply the aforementioned methods 1 and 2 to our uncertainty estimates to quantify potential biases due to the assumption of independence or due to the prescribed correlations in AR5. Throughout this study, we focus on projections from the mid-range emission scenario RCP4.5 for the period 2081–2100. Qualitatively similar results were found under the high emission scenario RCP8.5, and these results are included in the supplementary material.

2. Methods

Projections of RSL rise equal the sum of the individual components. Therefore, the uncertainty in these projections can be estimated from the uncertainty in the individual components through the following equation:

$$\sigma^2 \approx \sum_{i}^{N} \sigma_i^2 + 2 \sum_{i}^{N} \sum_{j>i}^{N} \rho_{i,j} \sigma_i \sigma_j \tag{1}$$

Here, σ is the standard deviation in the total sea-level rise, defined as the square root of the variance σ^2. This metric quantifies the uncertainty in the projected sea-level rise over a given time period. σ_i and σ_j are the standard deviations of the individual components i and j; and N is the total number of components constituting the total sea-level rise projection. $\rho_{i,j}$ is the correlation coefficient between components i and j, one of the critical variables to be quantified in this study. The first term on the right hand side is the sum of the individual variances (σ_i^2). The second term is the sum of the covariances between each unique set of components. As the correlations can equal any value between −1 and 1, the covariances can increase or decrease the total variance. Equation 1 is an approximation based on the assumption that all probabilistic distributions of the individual components are Gaussian. This is not necessarily the case for the distributions we develop throughout this study, but this equation is a useful approximation to diagnose the variances, correlations, and covariances.

In this study, we quantify the uncertainty in RSL projections by separately treating climate and process uncertainty. The climate uncertainty represents the uncertainty in regional climate change in response to greenhouse gas forcing; the process uncertainty represents the uncertainty in individual sea-level components to this change in regional climate. First, we extract the simulated climate change under RCP 4.5 or RCP 8.5 for a suite of 14 ESMs in the fifth coupled model intercomparison project (CMIP5). This simulated climate change encompasses all climate variables that impact the individual RSL components, as listed in Table 1. Next, the RSL contributions for each component are quantified based on these climate variables; this step is detailed for each sea-level component in the following subsections. This results in a multi-model ensemble of RSL projections for both the individual components and for the total RSL rise. We interpret the associated multi-model spread as the climate-uncertainty. We stress here that we do not aim to construct

Table 1
List of Regional Sea-Level Components for Which a Climate- and/or Process-Uncertainty is Determined

Contributor	Clim. unc.	Proc. unc.	Method	Primary reference
Sterodynamic	Yes	No	ESM output	N/A
Glaciers	Yes	Yes	Glacier model	Marzeion et al. (2012)
Greenland SMB	Yes	Yes	Parameterization	Fettweis et al. (2013)
Antarctic SMB	Yes	Yes	Parameterization	Gregory and Huybrechts (2006)
Antarctic dynamics	Yes	Yes	Parameterization	Levermann et al. (2020)
Greenland dynamics	No	Yes	AR5 values	Church et al. (2013)
Landwater storage	No	yes	AR5 values	Church et al. (2013)
Glacial isostatic adj.	No	yes	AR5 values	Church et al. (2013)

Note. For each component, a qualification of the method is added, together with the primary reference. Details on these methods to quantify uncertainties are found in Section 2.
Abbreviations: ESM, Earth system models; SMB, surface mass balance.

the most realistic RSL projections. Rather, we aim to construct projections which are consistent with the climate response of each ESM. The purpose of this ensemble is to construct a realistic multi-model spread in climate forcing, and resultant uncertainties, correlations, and covariances, from which the impact of correlations on RSL uncertainties can be quantified. This being said, we do find that our multi-model mean projections are close to those presented in AR5 (see Table S1). Finally, the total uncertainties are quantified by including the process-uncertainty for each component and each ESM. These process-uncertainties represent the uncertain relation between the climate forcing of the individual components and the resultant RSL contribution. In the remainder of this section, we describe in detail how these climate and process uncertainties are quantified based on ESM output. Furthermore, we describe how the correlations and covariances are diagnosed.

2.1. Sterodynamic

The first sea-level component is the sterodynamic change, following the terminology of Gregory et al. (2019). The sterodynamic component is an overarching term including the expansion or contraction of seawater due to changes in temperature and salinity (the steric component), the redistribution of ocean mass due to changes in ocean circulation (the dynamical part), and a correction for the inverse barometer effect. The sterodynamic component is explicitly included in the standard CMIP5 output, divided into a global mean and a purely regional term. In the global mean, steric expansion due to an increase in temperature dominates over changes in salinity (Gregory et al., 2019), and we therefore take the global mean thermosteric expansion (zostoga) which excludes the impact of global mean salinity change. In addition, the regional sterodynamic component (zos) describes regional deviations in density (thermal and haline) and mass. We detrend the global mean thermosteric expansion by removing the linear pre-industrial trend and subtracting the mean value over the reference period 1986–2005. This reference period is identical to that used for sea-level projections in AR5 and will be used throughout in this study. Next, we add the regional sterodynamic component, from which the annual global mean is removed to ensure consistency and prevent double counting of changes in global mean sterodynamic change. For each ESM, these regional time series are regridded to a common 1×1 degree grid. As the sterodynamic change is simulated explicitly by ESMs, we do not add any process-uncertainty for this component.

2.2. Glaciers

For glacier mass loss, a number of glacier models have been forced with output from different ESMs, as summarized in a recent model intercomparison study (GlacierMIP, Hock et al., 2019). From these different glacier models, the model of Marzeion et al. (2012) contains a substantial ensemble of ESMs (larger, for example, than the more recent study by Marzeion et al., 2020), and projections with this model under RCP4.5

are close to the multi-model mean. For these reasons, we take the glacier mass loss projections from this model as the glacier component in our ensemble.

The modeled glacier mass balance is a function of annual solid precipitation over the glacier surfaces and monthly mean air temperature at the elevation and location of the glacier termini. Additional ESM-independent terms contain climatological solid precipitation, a temperature-sensitivity of the glacier, and a bias correction. Modeled glacier mass loss is accumulated into 19 glacier regions from the Randolph Glacier Inventory (RGI Consortium, 2017). We convert their global sea-level contribution to regional values using the output from a Gravitation, Rotation, and Deformation (GRD) model (Milne & Mitrovica, 1998; Mitrovica et al., 2001; Tamisiea et al., 2010), assuming uniform mass loss for each individual region. The regional sea-level contributions are resolved on the same 1×1 degree global grid as the sterodynamic component. Again, the projections are referenced to the period 1986–2005.

The ESM ensembles in the aforementioned model intercomparison studies (Hock et al., 2019; Marzeion et al., 2020) are of insufficient size to explicitly derive both a climate- and a process-uncertainty. However, we can base our estimate for the process-uncertainty of glacier mass loss on these studies. Marzeion et al. (2020) performed an extensive uncertainty analysis on glacier projections, concluding that global climate- and process-uncertainties are largely independent and of similar magnitude. Ideally, we would determine process-uncertainties for individual glacier regions. The ensemble size of both ESMs and glacier models, however, varies across the glacier regions, which complicates the quantification of individual process-uncertainties. In addition, process-uncertainties for individual regions are likely to be co-dependent, though the correlation cannot be reliably estimated from the available ensemble. As a compromise, we approximate the process-uncertainty to be identical and equally distributed as the climate-uncertainty derived from our model ensemble. This process-uncertainty is assumed to be independent of all other uncertainties.

2.3. Greenland Surface Mass Balance

Two previous studies have explicitly simulated Greenland mass loss from an ensemble of ESMs (Fürst et al., 2015; Goelzer et al., 2020). However, these model ensembles are small and their overlap with the available ensemble for the glacier component is insufficient to compute statistically significant uncertainties and correlations. To ascertain a sufficient model ensemble size, we estimate future mass loss due to changes in Greenland surface mass balance (SMB) using the following parameterization (Fettweis et al., 2013):

$$\Delta SMB \approx \Delta SF - 84.2\Delta T - 2.4(\Delta T)^2 - 1.6(\Delta T)^3, \quad (2)$$

where ΔSF is the anomaly in annual snowfall over that part of the ice sheet where the elevation exceeds 1,000 m in the ESM-specific topography. This snowfall anomaly is multiplied with a factor 1.6, following Fettweis et al. (2013), to correct for ESM biases compared to regional climate models. ΔT is the anomaly in summer (JJA) atmospheric temperature at 600 hPa over the complete ice sheet. We have extracted these regional variables from the CMIP5 output for each ESM in our ensemble. Anomalies in temperature and snowfall are detrended by removing linear pre-industrial trends. The anomalies in SMB are then integrated over the historical and future period (1850–2100) to quantify the global contribution to sea-level change, which is again referenced to 1986–2005. Finally, the regional sea-level contribution is derived using similar GRD fields as applied to the glacier contribution, assuming uniform mass loss over the Greenland ice sheet. Note that a similar parameterization was provided by Fettweis et al. (2013) in terms of GMST, which was used in AR5 and SROCC to determine global mean uncertainties (Church et al., 2013; Oppenheimer et al., 2019).

We include a process-uncertainty for Greenland SMB based on the methodological uncertainty included in AR5. We follow the approach of AR5, as detailed by Palmer et al. (2020), and multiply ΔSMB by two factors, E and F. Factor E represents the increased mass loss due to the reduced surface elevation and is uniformly distributed between 1 and 1.15. Factor F represents the uncertainty in the above parameterization and is the exponent of a normal distribution with zero mean and a standard deviation of 0.4. The process-uncertainty of Greenland SMB is included by sampling 500 random values for E and F and multiplying ΔSMB with these for each ESM. The median RSL projections are taken as best estimates for each ESM in the quantification of the climate-uncertainty. Note that these best estimates are also affected by the inclusion of the process-uncertainty and deviate from the direct output of the above parameterization.

2.4. Antarctic SMB

Similar to Greenland SMB, we derive the sea-level contribution from changes in Antarctic SMB from a parameterization based on regional climate output of the different ESMs. This parameterization from Gregory and Huybrechts (2006) is based on the finding that net accumulation over the Antarctic ice sheet increases with regional atmospheric warming:

$$\Delta SMB = AP\Delta T. \tag{3}$$

Here, A is the time-mean snowfall accumulation during 1986–2005, equal to 1923 Gt yr^{-1} according to AR5. Factor P is the rate of increased accumulation per degree of regional atmospheric warming relative to this reference period, equal to 5.1% ± 1.5% per degree, and ΔT is the anomaly in atmospheric temperature averaged over the Antarctic ice sheet. Note that, again, a similar GMST-based parameterization was used in AR5 and SROCC, where a fixed ratio between GMST and Antarctic atmospheric temperature was prescribed. Here, we apply the parameterization to the regional atmospheric temperature as projected by the individual ESMs, detrended with respect to linear pre-industrial trends, instead. As for Greenland SMB, regional sea-level projections are based on output from the same GRD model, assuming uniform accumulation over the Antarctic ice sheet.

Again, we base the process-uncertainty for Antarctic SMB on the methodological uncertainty in AR5. First, we follow the assumption that the scaling factor P is normally distributed. Second, we multiply the net accumulation by a factor $(1 - S)$, representing the process correlation between Antarctic SMB and Antarctic dynamical mass loss. As detailed by Palmer et al. (2020), S is assumed to be uniformly distributed between 0 and 0.035. Both factors P and S are again sampled 500 times for each ESM, and the median RSL projection for each ESM is again taken as the best estimate for the climate-uncertainty. Note that we do not include the methodological uncertainty in Antarctic amplification from AR5 as we quantify Antarctic SMB from regional atmospheric temperature instead of GMST. This uncertainty is part of the climate-uncertainty rather than the process-uncertainty.

2.5. Antarctic Dynamics

For Antarctic dynamical mass loss, we use the recently published response functions by Levermann et al. (2020). These linear response functions are derived from idealized perturbation experiments with a suite of dynamical ice sheet models. Using these response functions, sea-level contributions from five Antarctic sectors can be found as a function of ocean temperature anomalies:

$$\Delta S(t) = \int_0^t \beta \Delta T_O R(t - \tau) d\tau. \tag{4}$$

Here, $S(t)$ is the sea-level rise contribution from dynamical mass loss of the Antarctic ice sheet. ΔT_O is the anomaly in ocean temperature in K, averaged spatially over one of five Antarctic regions and vertically over a depth of ±100 m around the mean depth of the ice shelves in each area. $R(t)$ is the nondimensional response function, specific per sector and per ice sheet model; specifically, we use the response functions derived from simulations with melt rates of 8 m yr^{-1}. β is the basal melt sensitivity, a prescribed parameter that relates ocean temperature to melt at the base of each ice shelf in m yr^{-1} K^{-1}.

Following Greenland and Antarctic SMB, we apply these parameterizations to regional ocean temperatures without scaling these to GMST. For each ESM, temperature anomalies are detrended by removing the trend over the period 1850–2000 and referenced to the average over this period. Referencing to this historical period suppresses the influence of unrealistic ocean variability in some ESMs during this period on the resultant sea-level projections. The integral is evaluated starting in the year 1850 and the derived sea-level contribution for each region is referenced to the mean value over 1986–2005. RSL contributions from the five Antarctic sectors are found by applying two regional fields from the GRD model. The regional imprint of mass loss from the Amundsen sector and the Antarctic peninsula are based on uniform mass loss from West Antarctica. The contribution from East Antarctica and the Weddell and Ross sector is distributed based on the assumption of uniform mass loss from East Antarctica.

The process-uncertainty for Antarctic dynamics is included following the uncertainty quantification by Levermann et al. (2020). We sample 500 random values for the basal melt sensitivity β, which is uniformly distributed between 7 and 16 m yr^{-1} K^{-1}. For each sample, we randomly select the response function R from one of the 16 ice sheet models. Again, the median result is taken as the best estimate for each ESM.

2.6. Other Components

Three more components contribute to RSL: Greenland dynamical mass loss, changes in land water storage, and glacial isostatic adjustment (GIA). For each of these components, we assess the total uncertainty to be dominated by process-uncertainty, and omit any climate-uncertainty. For the dynamical mass loss from the Greenland ice sheet, Slater et al. (2020) conclude that this contribution shows little variance when forced by atmospheric and oceanic variables from different ESMs. As of yet, no ESM-based simulations of changes in landwater storage are published, and the uncertainty in this contribution is primarily related to socio-economic aspects (e.g., Wada et al., 2016); we include this uncertainty as a process-uncertainty. Finally, glacial isostatic adjustment (GIA) contributes to RSL change, though it is independent of the climate system as defined in this study; that is: excluding the dynamic solid Earth system. Hence, these three components are excluded from our ESM ensemble and no climate-uncertainties are quantified for them. Rather, we include process-uncertainties, independent of all other components, which are equal to the regional uncertainty estimates in AR5. Note that in AR5, uncertainties are presented as likely ranges, whilst uncertainties in the underlying data set are expressed as standard deviations. For the use of AR5 uncertainties in our computations, and for the comparison of our results to those in AR5, we use standard deviations and variances throughout. Where necessary, likely ranges are converted to standard deviations by assuming Gaussian distributions.

2.7. Correlations

One central aim in this study is to quantify the correlation and covariance between RSL components. Here, we must distinguish between two types of correlation. The first is the *climate correlation* which is induced by the co-dependence in climate forcing between the different sea-level components. The second is the *total correlation*, which is the correlation that applies to the total uncertainty. Here, we describe how these two types of correlation can be diagnosed.

The climate correlation is the correlation coefficient in the formula for climate uncertainty:

$$\sigma_c^2 \approx \sum_i^N \sigma_{ci}^2 + 2\sum_i^N \sum_{j>i}^N \rho_{ci,j}\sigma_{ci}\sigma_{cj}. \tag{5}$$

This is the equivalent of the general Equation 1 for climate uncertainty. σ_c denotes the climate uncertainty, and ρ_c the climate correlation. As argued based on the statistical analysis of Le Bars (2018), the rank correlation, also Spearman's correlation, is an appropriate estimate of the correlation between quasi-Gaussian uncertainties. In this study, we quantify the climate correlation as the rank correlation across the ESM ensemble. Multiplying this correlation with the climate-uncertainties of the individual components gives the covariance, which complements the climate-uncertainty in RSL projections. We will use the climate correlation to identify physical mechanisms behind the co-dependence between RSL components.

An equivalent correlation is given in Equation 1 for the total uncertainty: $\rho_{i,j}$. This correlation is quantified as the rank correlation across the full ensemble for all components, including the process-uncertainty. Hence, this correlation is based on a total of 7,000 values (14 ESMs times 500 samples). This total correlation provides us with little new physical insight compared to the climate correlation. Yet it is a useful metric to compare our study to the three methods described in the introduction: the assumption of independence is equivalent to a total correlation of 0; the prescribed correlations in the RSL uncertainty estimates of AR5 are applied to the total uncertainty and can thus be interpreted as total correlations; and Palmer et al. (2020) diagnosed the total GMST-based correlation that was implicit in the AR5 method for global sea-level projections. In the next section, we will compare our total correlations to those resulting from these three methods.

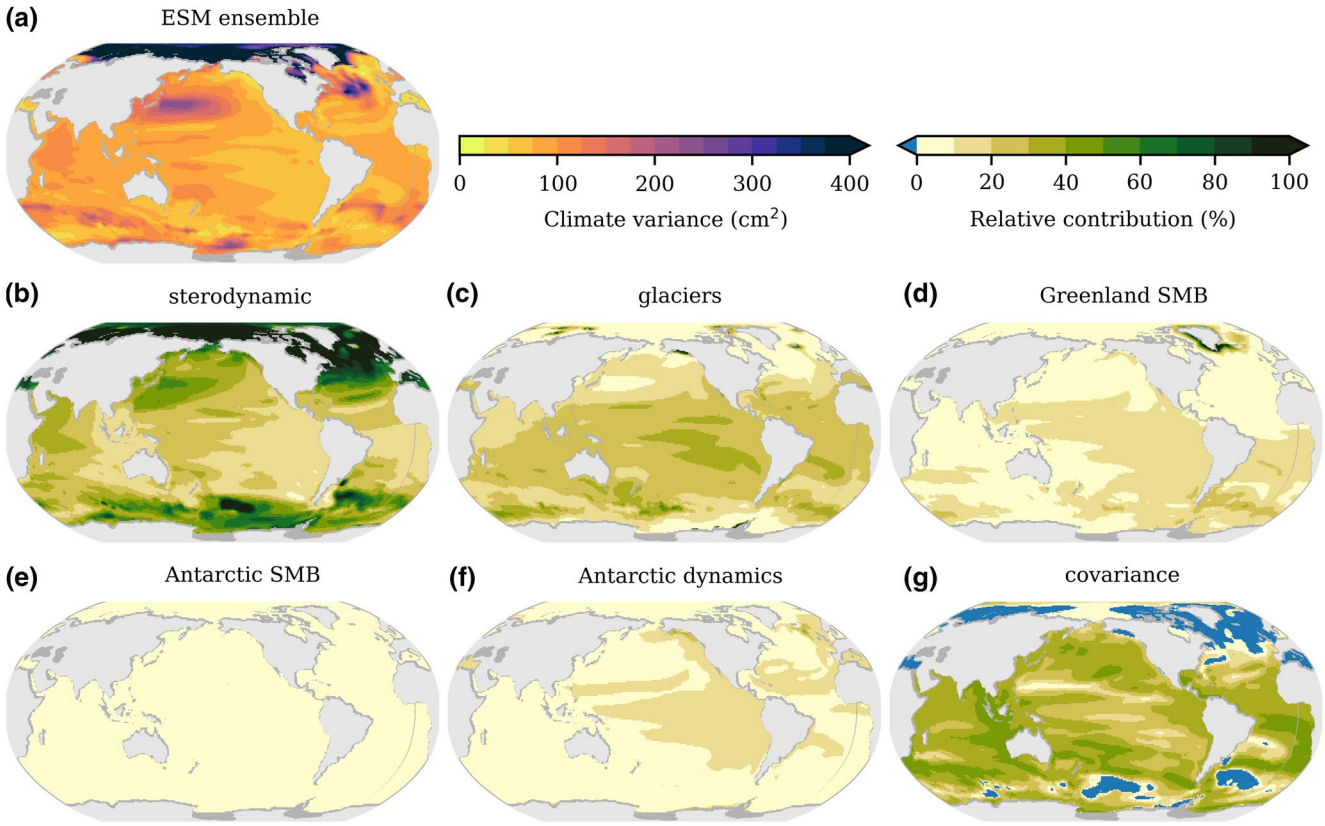

Figure 1. Regional climate variance and its decomposition. These panels are the regional counterparts of the global climate variances in Table SI.1. (a) The climate variance σ_c^2 in the RSL projections across the 14 ESMs (Figure SI.1). (b–f) The climate variances for the individual components σ_{cli}^2, scaled to the total climate variance in (a) at each grid point. (g) The total contribution from covariance. Negative values here imply that negative correlations between sea-level components lead to a net reduction in the total variance. The sum of (b–g) add up to 100% at each grid point. ESM, Earth system models; RSL, regional sea-level.

3. Results

The results section is organized as follows. First, we discuss the ESM ensemble of global and regional sea-level projections. Based on this ensemble, we discuss the climate uncertainty, climate correlation, and climate covariance in RSL. Next, we present the total RSL uncertainty and the total correlation, which are compared to previous works. Finally, we apply previously published correlations to our uncertainty estimates. This allows for the quantification of errors in RSL uncertainty due to prescribed correlations.

3.1. Climate Uncertainty

Global mean sea-level projections under RCP4.5 for 2081–2100 are listed in Table S1 for our ensemble of 14 ESMs. The ensemble mean contributions agree well with those listed in AR5, indicating that our method is line with the method in AR5, and our ESM ensemble is representative for the complete CMIP5 ensemble. The primary difference is that our estimate of the ensemble mean glacier contribution is slightly higher in our ensemble compared to AR5. The regional climate uncertainty in total sea-level rise displays a large spatial heterogeneity (Figure 1a). This figure equals the multi model variance of the ESM ensemble, shown in Figure S1. The largest climate uncertainty is found in the Arctic Ocean, the subtropical gyres, and several spots in the Southern Ocean.

As expressed in Equation 5, the total climate variance equals the sum of the individual variances, plus the total covariance. Both globally and regionally, the individual components of sterodynamic change and glaciers dominate the climate uncertainty (Table S1, Figures 1b and 1c). The large uncertainty in the Arctic stems from the disagreement between ESMs on the rate of sea-ice decline and is reflected in the large

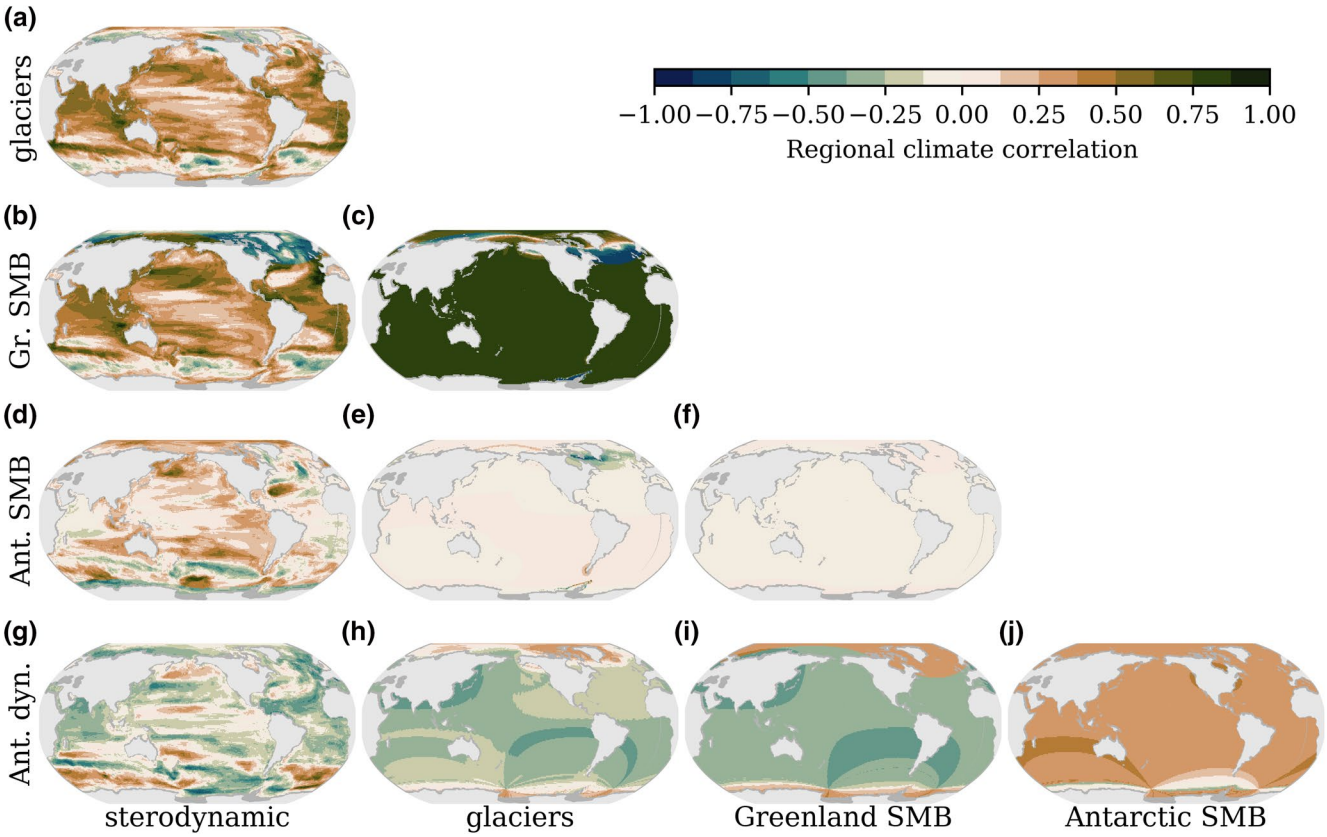

Figure 2. Regional climate correlation $\rho_{cli,j}$ for each unique set of sea-level components i and j. Positive (negative) values indicate that the correlation has the potential to increase (decrease) the total climate variance.

uncertainty in the sterodynamic component (Figure 1b). Also the high uncertainties in the subtropical gyres and the Southern Ocean can be traced back to the sterodynamic component and are related to uncertain changes in ocean dynamics (e.g., Little et al., 2015). The uncertainty in the glacier contribution is primarily expressed in the far-field (sub)tropics and nearby glacier regions such as Alaska, due to the GRD imprint of its mass loss.

In addition to these individual variances, the covariance accounts for approximately 1/3 of the total climate variance in global mean sea-level projections (Table S1). Regionally, this contribution varies between negative values, primarily in the higher latitudes, up to 50% in the lower latitudes. The climate covariance equals the product of the climate uncertainty of two sea-level components $\sigma_{cli}\sigma_{clj}$, multiplied by the correlation between these components $\rho_{cli,j}$ (see Equation 1). The significant contribution of covariance to the total climate uncertainty σ_c thus illustrates the importance of an accurate estimate of the climate correlations, both on a global and a regional level.

3.2. Climate Correlation

The climate correlation is computed as the rank correlation in RSL contributions across the ESM ensemble. These correlations are presented in Figure 2 and display a strong regional variability. The climate correlation between the sterodynamic component and all others (Figures 2a, 2b, 2d, and 2g) is marked by relatively small-scale features related to changes in ocean density and circulation (e.g., Gregory et al., 2019). Whereas the sterodynamic and glacier components have a climate correlation of 0.5 in their contributions to global mean sea-level (not shown), regionally, this correlation is smaller nearly everywhere (Figure 2a). This difference between global and regional correlations indicates that changes in ocean dynamics, and regional sterodynamic change in general, are partially decoupled from the global mean thermosteric expansion. As

a consequence that was also noted by Palmer et al. (2020), global correlations cannot be directly applied regionally as was done in AR5.

The problem with the direct application of global correlations is even more prominent when the sign of RSL contributions varies regionally. This is the case nearby ice masses, where mass loss induces a regional sea-level drop due to the change in the gravitational field (e.g., Mitrovica et al., 2001). Whilst the correlation between the global sterodynamic and Greenland SMB components is positive, the regional correlation is negative nearby the Greenland ice sheet (Figure 2b). A larger than expected thermosteric expansion will typically coincide with a larger mass loss due to changes in Greenland SMB. The former leads to an enhanced RSL rise nearby the Greenland ice sheet, while the latter leads to an enhanced negative RSL contribution. These effects partially cancel at regional scales, illustrating how negative regional correlations reduce the total uncertainty in RSL.

The ice mass components generally exhibit globally consistent correlation patterns, except near their ice mass source. The climate correlation between glaciers and Greenland SMB, for example, is near 1 globally, except in regions where either component induces a net sea-level drop (Figure 2c). This near-perfect climate correlation results from the shared dependency on regional temperature and snowfall, predominantly in the Northern Hemisphere higher latitudes (Goelzer et al., 2020; Marzeion et al., 2020). Climate correlations related to Antarctic SMB are minor (e.g., Figures 2e and 2f), except for the positive correlation with Antarctic dynamics (Figure 2j). Enhanced ocean warming around the Antarctic ice sheet results in increased dynamic Antarctic ice mass loss, and is correlated with a reduced increase in snowfall (a less negative sea-level contribution from Antarctic SMB). This positive correlation thus represents an anti-correlation between oceanic and atmospheric warming near the Antarctic ice sheet. The negative climate correlation between Antarctic dynamics and both glaciers and Greenland SMB (Figures 2h and 2i) reflects the overall negative climate correlation between Antarctic dynamics and GMST (not shown).

Another notable pattern is the highly regional climate correlation between the sterodynamic and Antarctic dynamic components (Figure 2g). Spatial variations are visible, most clearly in the Atlantic basin. A positive correlation is observed in the Southern Ocean, contrasting a negative correlation most pronounced in the North Atlantic and Nordic Seas. This pattern illustrates the impact of the large-scale ocean circulation and heat distribution on regional climate correlations. If more heat is accumulated in the Southern Ocean, this results in both a larger regional sterodynamic contribution and a larger mass loss due to Antarctic dynamics: a positive correlation. The dipole pattern in the Atlantic basin hints at a role for the Atlantic Meridional Overturning Circulation (AMOC), which maintains a heat transport toward the North Atlantic and the Nordic Seas. A weakening of this circulation would lead to northern cooling and hence a reduction in the regional thermosteric expansion. At the same time, it redirects excess heat toward the Southern Ocean leading to an increase in Antarctic dynamic mass loss. Altogether, the climate correlation is found to be strongly regional, and many of these regional features cannot be traced back directly to the GMST-dependence of individual sea-level components. Instead, they are induced by regional climate processes.

The contribution of climate correlations to the total climate variance is quantified by the covariances (the last term in Equation 5). These covariances are visualized as regional fields in Figure 1 in terms of their relative contribution to the total climate variance (Figure 3a). Hence, the sum of these covariances is equal to the total climate covariance displayed in Figure 1g. The regional sign of each covariance is necessarily equal to the sign of the corresponding regional correlation, as each standard deviation σ is positive.

These separate covariances can help us to understand the net contribution of the correlations to the total climate uncertainty. In the lower latitudes, the covariances are primarily positive, leading to an increase in the total climate uncertainty. This is in agreement with the global contribution of the covariance which accounts for 1/3 of the total climate variance, as discussed above. However, a number of regional exceptions are seen. In the Northern polar regions, several covariances are negative, which can be attributed to the negative RSL contribution of the different ice masses. Another exception is the Mediterranean Sea, where the total climate covariance is negative. The covariance between the sterodynamic component and mass loss from glaciers and Greenland SMB is negligible, implying that the sterodynamic component in the Mediterranean is independent of global thermosteric expansion and GMST. A negative correlation, though, is found between the sterodynamic component and Antarctic dynamics. This is again likely related to the

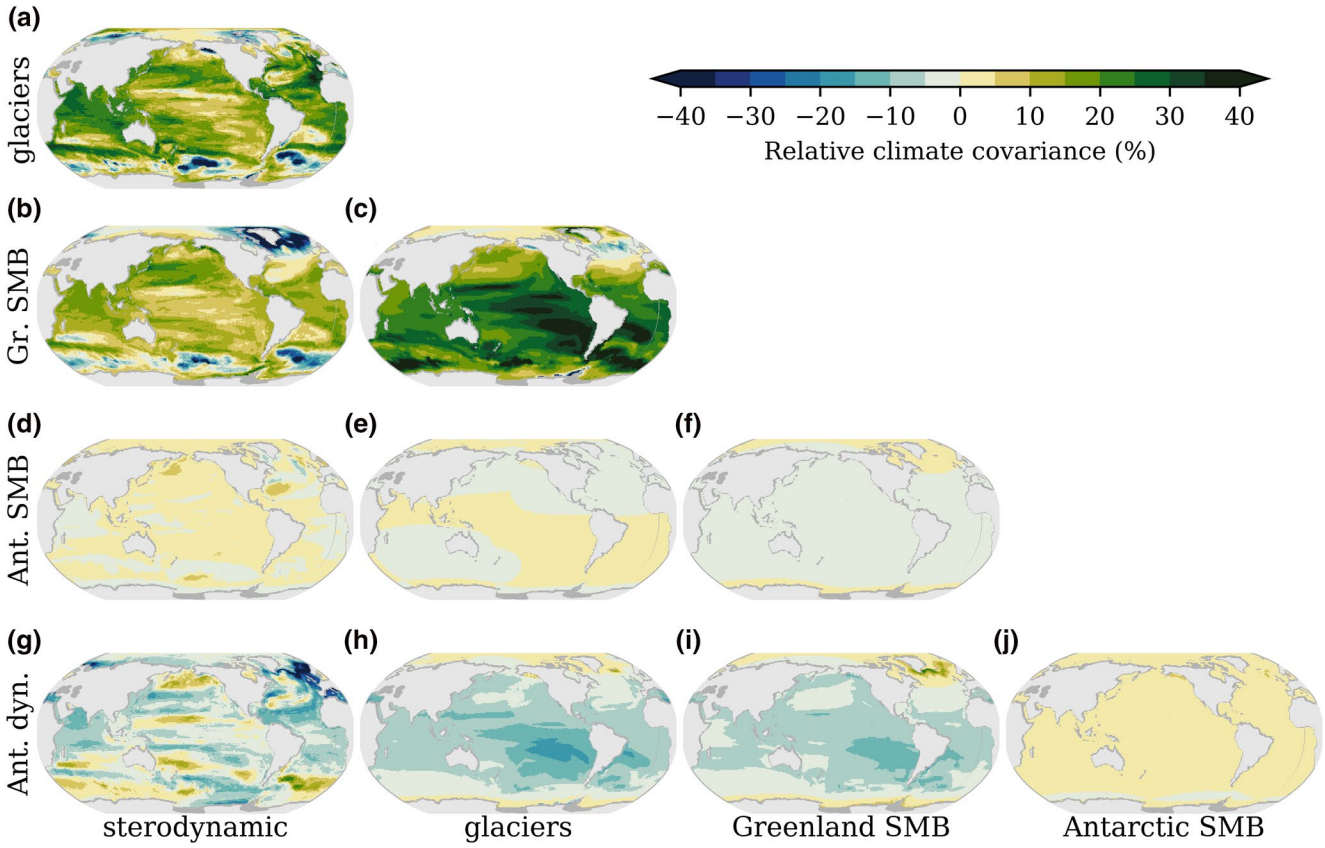

Figure 3. Contribution of covariances to the total climate variance. Each panel denotes the covariance $2\rho_{c\mathrm{l}i,j}\sigma_{c\mathrm{l}i}\sigma_{c\mathrm{l}j}$ in Equation 5, scaled to the total climate variance σ_c^2 at each grid point. These fields are the multiplication of the climate correlations in Figure 2 and the associated standard deviations from Figure 1. The sum of these fields equals that in Figure 1g.

response of the large-scale ocean circulation. The resultant negative covariance reduces the total climate variance in this region, hence reducing the uncertainty of RSL in the Mediterranean due to the uncertain climate response to greenhouse gas forcing.

3.3. Total Uncertainty

The inclusion of process uncertainties allows for the quantification of the total uncertainty for each individual sea-level component (Figure 4). As mentioned above, the total variance in the sterodynamic component is equal to its climate variance, as this component is explicitly simulated by the ESMs. The glacier variance is double the glacier component's climate variance, increasing its contribution to total RSL uncertainty. Notably, the total variance in Antarctic dynamics is of comparable magnitude to the glacier variance, despite its relatively moderate climate variance (Figure 1f). The large uncertainty in the basal melt sensitivity β (Equation 4) and the large spread in response functions R between ice models introduces a large process uncertainty. In addition, the three components that were not included in our ESM ensemble show large regional variances (Figures 4f–4h).

The total variance in RSL, including both climate and process uncertainties of all components as well as all covariances, is shown in Figure 5a. Similar spatial patterns are observed to the climate variance (Figure 1a), though the overall magnitude is greater. Globally, the total variance is of comparable magnitude to that found in AR5 (Figure 5b), though large regional differences are observed (Figure 5c). In the Arctic, the total variance in this study is more than twice as large as in AR5. This is again likely related to the ESM-spread in projected Arctic sea-ice decline. Regional differences, both positive and negative, are found throughout the subtropical basins and the Southern Ocean, related to ocean dynamics. In addition, regional differences

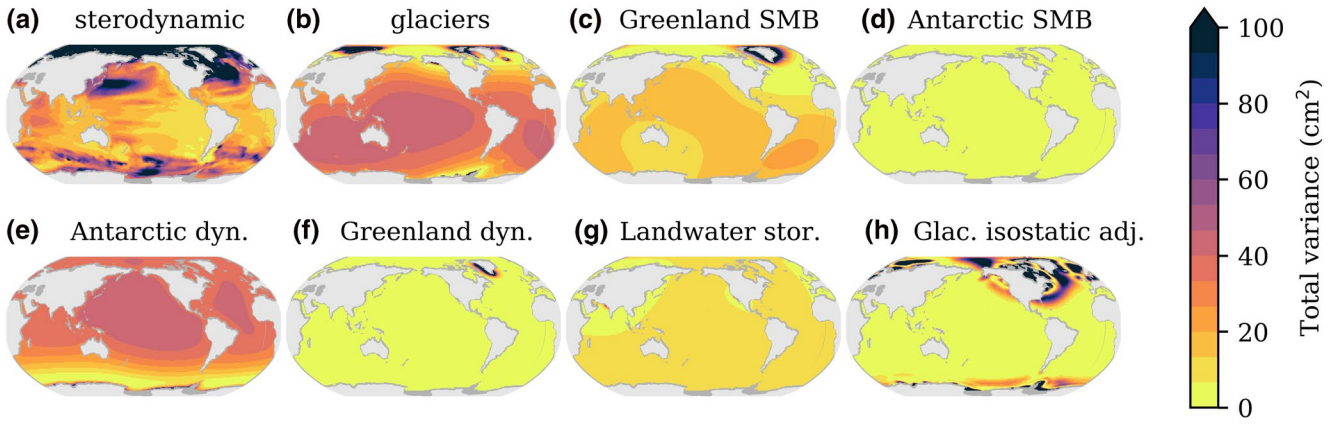

Figure 4. Total variance σ_i^2 for each individual sea-level component. This total variance includes both the climate and process uncertainty in accordance with Table 1.

are observed near glacier regions including Alaska and South America. These glacier-related differences may result from differences in the assessed glacier uncertainty, or from differences in glacier-related correlations. Both differences related to sea-ice and ocean dynamics depend on the ESM ensemble, which differs between our study and AR5. Usage of the same ensemble would likely reduce these differences.

In the North Atlantic and the Nordic Seas and around the Antarctic Peninsula, the total variance in this study is less than that in AR5 (Figure 5c). We attribute the discrepancy in the North, up to 50%, to the negative covariance between the sterodynamic component and both the Greenland SMB and Antarctic dynamic components (Figures 3b, 3d, and 3g). These impose a net negative contribution of the covariance to the climate uncertainty in this region (Figure 1g). As discussed above, these negative covariances are due to negative correlations between regional sterodynamic change and ice mass loss through their dependencies on the large-scale ocean circulation. The discrepancy around the Antarctic Peninsula, regionally more than 100%, originates from differences in the distribution of Antarctic dynamic mass loss. In AR5, most mass loss is attributed to the Amundsen sector, while in our study based on Levermann et al. (2020), Antarctic dynamic mass loss is more evenly distributed over the different sectors. The spatial imprint, related to a near-field sea-level drop is therefore less pronounced in this study, leading to a smaller uncertainty in this region.

3.4. Total Correlation

To compare our total correlations $\rho_{i,j}$ to previous studies, we focus on the global correlations. In AR5, uncertainties in RSL were determined through the ad-hoc prescription of global correlations of either 0 or 1, as displayed in Figure 6a. Uncertainties in global mean sea-level projections were found through the propagation of GMST-dependencies of the individual components. The implicit correlations were quantified by Le Bars (2018) and Palmer et al. (2020) and are displayed in Figure 6b. A most notable difference

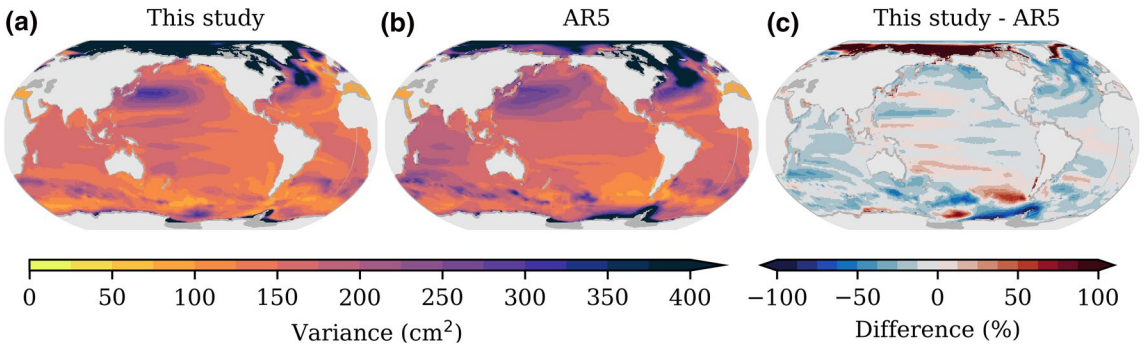

Figure 5. Total regional variance σ^2 in this study (a) compared to AR5 (b) (Church et al., 2013). (c) The difference in variance between these two studies.

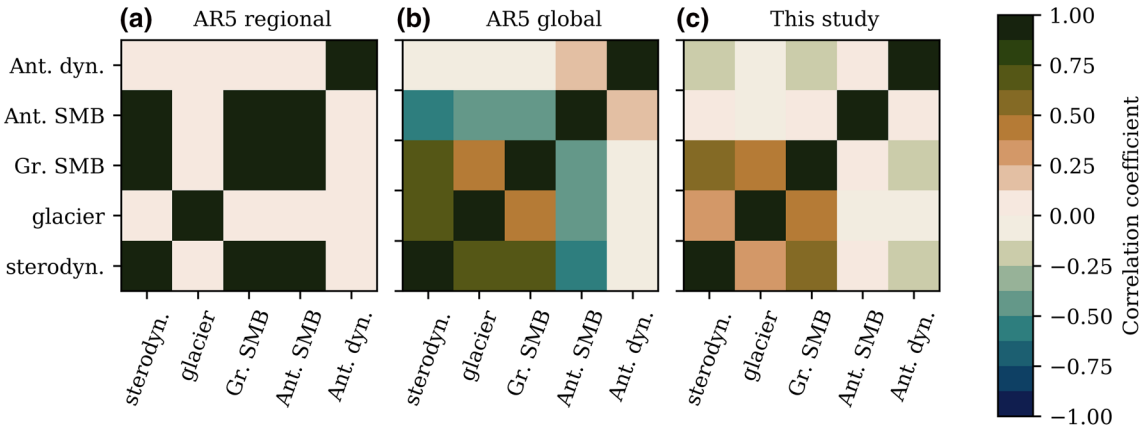

Figure 6. Total correlation coefficients $\rho_{i,j}$, compared to AR5 (Church et al., 2013). (a) Prescribed correlations in the regional uncertainty estimate of AR5, referred to as 'method 1' in this study. (b) The global AR5 correlations as derived from Palmer et al. (2020). (c) The global correlations in this study.

in global correlations is found for Antarctic SMB. Regionally, correlations of 1 were applied between the uncertainties in Antarctic SMB and Greenland SMB and sterodynamic change (Figure 6a). Globally, these correlations are negative, as the net contribution of Antarctic SMB is negative and a relation between Antarctic atmospheric temperature change and GMST was prescribed (Figure 6b). In our study, however, we find negligible correlations between Antarctic SMB and the other components, as we find no clear link between GMST and regional atmospheric temperature over the Antarctic continent (Figure 6c). Though these differences are large in terms of correlations, we should stress that the uncertainty in Antarctic SMB is small (Table S1), so its impact on the total covariance and total uncertainty is small as well.

Another marked difference in correlations is that between sterodynamic change and glaciers. In the RSL computations of AR5, these components were assumed to be independent. In the global mean sea-level projections, however, a strong positive correlation was found. The global climate correlation between these components in this study is less than that derived from the GMST-based method (not shown), as glacier mass loss is based on regional atmospheric temperature and snowfall (Marzeion et al., 2012) rather than GMST. The total correlation is reduced further as the process uncertainty in the glacier component is independent of the climate uncertainty. Because the uncertainties in sterodynamic change and glacier mass loss are among the largest uncertainties (Table S1), this discrepancy in correlations has a considerable impact on the covariance and the total uncertainty. In general, we can conclude that the total global correlations in this study are predominantly positive and of moderate magnitude compared to the regional and global correlations in AR5.

The difference in correlations affects the resultant RSL uncertainty estimates. To quantify this impact, we apply the correlations $\rho_{i,j}$ from two previously adopted methods to our individual uncertainties σ_i to compute the total uncertainty σ. These methods were described in the introduction as methods 1 (the assumption of independence) and method 2 (the prescribed mixture of independence and perfect codependence as in AR5, see Figure 6a). The resultant total variances are shown in Figures 7a and 7b. In Figures 7c and 7d, these total variances are compared to the actual total variance in this study, and expressed in terms of a relative error. As correlations are predominantly positive in this study, the assumption of independence leads to an overall underestimation of RSL uncertainties, which is in the order of 20%. Overestimations are found in the high latitude regions and the Mediterranean Sea, where a net negative covariance reduces the total RSL uncertainty (Figure 1g).

The correlations prescribed in the RSL computations in AR5 are found to overestimate the total variance (Figure 7d). As no negative correlations are applied in this method, overestimations should be expected in the regions with a negative climate covariance. These overestimations exceed 100% regionally. Globally, overestimations are found to be in the order of 20%. In the lower latitudes, methods 1 and 2 therefore produce errors of similar magnitude but opposite sign, approximately −20%. In the higher latitudes and the Mediterranean, method 2 leads to a greater overestimation as this method does not account for regional

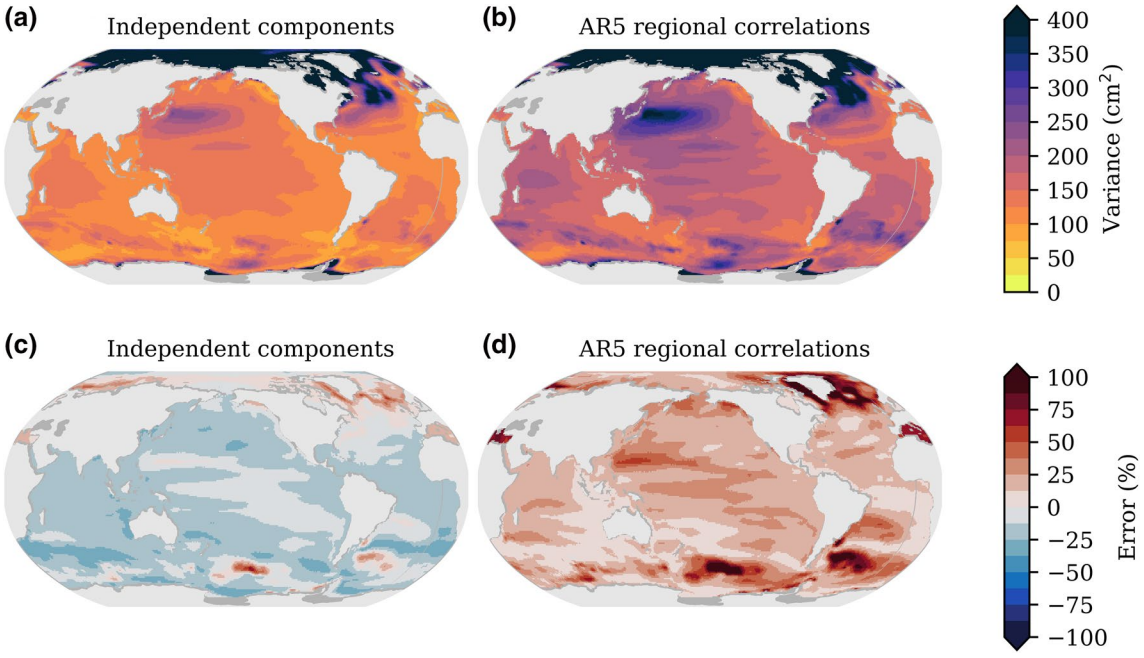

Figure 7. Estimates of total variance based on two methods, applied to the individual uncertainties σ_i from this study (Figure 4). (a and c) The total variance based on the assumption of independence, that is, $\rho_{i,j} = 0$. (b and d) The total variance based on method 2, where the same correlations are applied as in the AR5 regional estimates (Figure 6a). (a and b) The total variance. (c and d) The error in total variance relative to the total variance estimated in this study (Figure 5a).

negative correlations related to dependencies on the large-scale circulation and the near-field sea-level drop due to ice mass loss.

4. Discussion

In this study, we have computed uncertainties in regional sea-level projections based on an ensemble of Earth System Models. We have distinguished between the uncertainty due to the climate's response to greenhouse gas forcing (the climate uncertainty) and the response of individual sea-level components to this climate change (the process uncertainty). The choice of the underlying model ensemble impacts the estimates of the uncertainties and this choice is a trade-off between a large ensemble size and a realistic translation from regional climate change to sea-level contributions. As no parameterization is available for regional glacier mass loss, our ensemble is limited by the available ESM ensemble for which regional glacier projections have been performed. To ensure a sufficient ensemble size, we have chosen to apply a parameterization for Greenland SMB change rather than model projections based on a small ensemble size (e.g., Fürst et al., 2015; Goelzer et al., 2020), as these latter ensemble sizes were deemed insufficient. Our results thus depend inevitably on the model performance of our chosen ESM ensemble. In addition, our results rely on a number of parameterizations, which represent our limited knowledge of the climate-dependency of sea-level components. Ideally, our methodology would be applied to explicit model projections of all sea-level components, rather than parameterizations, based on a substantial ensemble of ESMs to optimize both the realism as well as the ensemble size. At the moment of writing, such model projections are not available.

While we have aimed for a realistic assessment of climate uncertainty, our treatment of process uncertainties can be classified as idealized. The exception is the process uncertainty in Antarctic dynamical mass loss, which is based on an ensemble of 16 ice sheet models and we can be confident that this process uncertainty is relatively well sampled. However, a similar approach was not possible for all sea-level components as, again the availability of explicit projections with, for example, glacier models is insufficient. Again, an increased ensemble of model projections both in terms of ESMs and ice sheet models would improve the realism of process uncertainties and hence the estimates of total RSL uncertainty using our method.

Taking into account, more realistic process uncertainties would also allow for a more realistic treatment of correlations between climate and process uncertainties. We have included such correlations by propagating uncertainties from regional climate change to sea-level contributions. Projections of large contributions from Greenland and Antarctic SMB and Antarctic dynamics, based on "warm" ESMs, are associated with relatively large process uncertainties. In other words, process uncertainties depend on climate uncertainties and this dependence is represented by our approach. However, we have treated the process uncertainties between the different sea-level components as independent, which may not be the case. The negative correlation between Antarctic SMB and Antarctic dynamics is represented by the factor $(1 - S)$, but other process correlations may exist. All SMB terms including glacier mass loss depend on common uncertain process such as the melt-albedo feedback. If this feedback enhances and/or skews the uncertainty in sea-level contributions, this would apply to all relevant components, hence introducing a correlation. A similar argument can be made for ice dynamical contributions from the Greenland and Antarctic ice sheets which depend on similar processes. The realistic inclusion of process correlations could further improve our methodology and improve the accuracy of regional sea-level uncertainty estimates.

In this study, we have diagnosed correlations from the model ensemble of sea-level contributions. As our ensemble size is limited, we have only focused on correlations that apply to the bulk distributions, assuming Gaussian distributions for all components. Different correlations may apply, however, to the tail distributions (e.g., Bamber et al., 2019). Such tail dependencies are particularly important for high-end estimates (Le Bars, 2018). The quantification of tail correlations would require a large ensemble size and an accurate representation of non-linearities in process uncertainties. Again, we recommend this as an improvement upon our methodology when more model projections are available.

The comparison of our RSL uncertainty estimates to previous methodologies, AR5 in particular, illustrates a number of issues regarding the application of globally uniform correlations to regional uncertainty estimates. First, the negative RSL contribution near ice masses must be accounted for in the application of regional correlations. This can be done through a direct scaling or by applying a Monte Carlo-based approach as done by Palmer et al. (2020). Second, the partial decoupling between global and regional sterodynamic contributions must be accounted for. Although the regression-based scaling by Palmer et al. (2020) does address this issue, it is based on a regression calculated per ESM. However, the decoupling arises from the cross-ESM disagreement and the scaling between global and regional codependencies should be derived from a cross-ESM regression (equivalent to our climate uncertainty). Third, alternatives should be found for the GMST-based quantification of correlations. The GMST-based method is a first-order approach to quantify climate correlations and we find that it results in inaccurate correlations, both globally and regionally. As an example of GMST-independent physical mechanisms that introduce climate correlations between sea-level components, we have identified the large-scale ocean circulation. Changes in this circulation redistribute heat, affecting ice mass loss as well as regional sterodynamic change. This mechanism imposes regional climate correlations between sterodynamic change and Antarctic dynamics up to −0.5 in the North Atlantic and the Nordic Seas. The global correlation between these components is negligible, and hence any global variable such as GMST is a poor indicator for this regional correlation.

The identification of this physical mechanism illustrates the general usefulness of our ensemble-based methodology. By constructing sea-level projections that are consistent with the projected climate change by a suite of ESMs, we have identified a teleconnection between regional sterodynamic change and Antarctic mass loss. This mechanism is identified based on the multi-model spread rather than the ensemble mean or the simulations with individual models. We believe focusing on inter-model disagreement, rather than inter-model agreement, can provide new insight in physical mechanisms that are difficult to identify from individual models. This approach can be applied to any climate-related subject beyond regional sea-level rise.

5. Conclusions

In this study, we have quantified the uncertainty in regional sea-level based on a model ensemble of regional climate change projections. The quantification of total uncertainty was based on the propagation of the uncertainty in the regional climate response to greenhouse gas forcing, to the uncertainty in the response of sea-level components to this regional climate change. Global values of multi-model mean sea-level

projections and the climate variance of individual components agreed well with those reported in AR5. The regional climate variance is dominated by the variance in regional sterodynamic change in the higher latitudes and by the variance in glacier mass loss and covariance between the different components in the lower latitudes. In the higher latitudes, this covariance was found to be largely negative, due to negative regional correlations between the different components.

Negative regional correlations arise from the near-field sea-level drop due to ice mass loss, from the co-dependence between regional ocean dynamics in the Southern Ocean and global heat uptake, and from the teleconnection between regional sterodynamic change, particularly in the North Atlantic and Nordic Seas, and Antarctic dynamical mass loss. This teleconnection is likely related to the large-scale ocean circulation that regulates the heat distribution between the Southern Ocean and the northern oceans. These mechanisms illustrate that correlations between sea-level components are governed by the coupled climate system and regional changes therein, rather than by a global indicator such as global mean surface temperature. They further illustrate that the application of globally uniform correlations to regional uncertainties leads to biases in the total regional sea-level uncertainty.

The correlations in the regional sea-level estimates of AR5 lead to a global overestimation on the order of 20%. Regionally, this overestimation exceeds 100%, in particular near ice masses, in the Southern Ocean, and in the Mediterranean Sea. These are the regions where negative correlations between sea-level components reduce the total uncertainty. Computations for the high emission scenario RCP 8.5, presented in the Supplementary Information, reveal an equivalent overestimation in relative terms. On a global scale, we conclude that the assumption of independence is more accurate than the prescribed mixture of independence and perfect codependence as done in AR5. Again, this conclusion is independent on the emission scenario. More generally, regional variations in the correlation must be accounted for in order to quantify realistic uncertainties in regional sea-level projections. These regional variations cannot accurately be derived from the dependence on global mean surface temperature, as physical mechanisms in the climate system such as the large-scale ocean circulation play a crucial role in establishing these correlations. Dynamical processes such as heat distribution, precipitation patterns and ocean circulation govern regional sea-level change and these cannot be extracted directly from any global indicator such as global mean surface temperature. We therefore conclude that, in the assessment of correlations between sea-level components—and climate change in general—the climate system should be acknowledged and treated as an inherently coupled system.

Data Availability Statement

The code underlying this work is available at https://github.com/erwinlambert/codependence. The data that support our findings are available in the open repository http://doi.org/10.5281/zenodo.4049932

Acknowledgments
Erwin Lambert has received funding from the INSeaPTION project which is part of ERA4CS, an ERA-NET initiated by JPI Climate, and funded by NWO with co-funding by the European Union (Grant 690462). Dewi Le Bars received funding from the European Union's Horizon 2020 research and innovation programme under the grant agreement RECEIPT No 820712. Heiko Goelzer has received funding from the programme of the Netherlands Earth System Science Center (NESSC), financially supported by the Dutch Ministry of Education, Culture and Science (OCW), under grant no. 024.002.001. The authors thank T. Frederikse for providing output from the GRD model. Finally, the authors thank two anonymous reviewers for their constructive comments.

References

Bamber, J. L., Oppenheimer, M., Kopp, R. E., Aspinall, W. P., & Cooke, R. M. (2019). Ice sheet contributions to future sea-level rise from structured expert judgment. *Proceedings of the National Academy of Sciences of the United States of America*, *116*(23), 11195–11200. https://doi.org/10.1073/pnas.1817205116

Barthel, A., Agosta, C., Little, C. M., Hattermann, T., Jourdain, N. C., Goelzer, H., et al. (2020). Cmip5 model selection for ismip6 ice sheet model forcing: Greenland and Antarctica. *The Cryosphere*, *14*(3), 855–879. https://doi.org/10.5194/tc-14-855-2020

Carson, M., Köhl, A., Stammer, D., Slangen, A. B. A., Katsman, C. A., van de Wal, R. S. W., et al. (2015). Coastal sea level changes, observed and projected during the 20th and 21st century. *Climatic Change*, *1341–2*, 269–281. https://doi.org/10.1007/s10584-015-1520-1

Church, J., P. Clark, A. Cazenave, J. Gregory, S. Jevrejeva, A. Levermann, et al. (2013). Sea level change. In T. Stocker, D. Qin, G.-K. Plattner, M. Tignor, S. Allen, J. Boschung, et al. (Eds).*Climate change 2013: The physical science basis. Contribution of working group I to the fifth assessment report of the intergovernmental panel on climate change* (pp. 1137–1216): Cambridge University Press.

Eyring, V., Bony, S., Meehl, G. A., Senior, C. A., Stevens, B., Stouffer, R. J., & Taylor, K. E. (2016). Overview of the coupled model intercomparison project phase 6 (cmip6) experimental design and organization. *Geoscientific Model Development*, *9*(5), 1937–1958. https://doi.org/10.5194/gmd-9-1937-2016

Fettweis, X., Franco, B., Tedesco, M., van Angelen, J. H., Lenaerts, J. T. M., van den Broeke, M. R., & Gallée, H. (2013). Estimating the Greenland ice sheet surface mass balance contribution to future sea level rise using the regional atmospheric climate model mar. *The Cryosphere*, *7*(2), 469–489. https://doi.org/10.5194/tc-7-469-2013

Fürst, J. J., Goelzer, H., & Huybrechts, P. (2015). Ice-dynamic projections of the Greenland ice sheet in response to atmospheric and oceanic warming. *The Cryosphere*, *9*(3), 1039–1062. https://doi.org/10.5194/tc-9-1039-2015

Garner, A. J., Weiss, J. L., Parris, A., Kopp, R. E., Horton, R. M., Overpeck, J. T., & Horton, B. P. (2018). Evolution of 21st century sea level rise projections. *Earth's Future*, *6*(11), 1603–1615. https://doi.org/10.1029/2018ef000991

Goelzer, H., Nowicki, S., Payne, A., Larour, E., Seroussi, H., Lipscomb, W. H., et al. (2020). The future sea-level contribution of the Greenland ice sheet: A multi-model ensemble study of ismip6. *The Cryosphere 14*(9), 3071–3096. https://doi.org/10.5194/tc-14-3071-2020

Gregory, J. M., Griffies, S. M., Hughes, C. W., Lowe, J. A., Church, J. A., et al. (2019). Concepts and terminology for sea level: Mean, variability and change, both local and global. *Surveys in Geophysics*, *40*(6), 1251–1289. https://doi.org/10.1007/s10712-019-09525-z

Gregory, J. M., & Huybrechts, P. (2006). Ice-sheet contributions to future sea-level change. *Philosophical Transactions of the Royal Society A: Mathematical, Physical and Engineering Sciences*, *364*(1844), 1709–1731. https://doi.org/10.1098/rsta.2006.1796

Grinsted, A., Jevrejeva, S., Riva, R. E. M., & Dahl-Jensen, D. (2015). Sea level rise projections for northern Europe under rcp8.5. *Climate Research*, *64*(1), 15–23. https://doi.org/10.3354/cr01309

Hall, J. A., Weaver, C. P., Obeysekera, J., Crowell, M., Horton, R. M., Kopp, R. E., et al. (2019). Rising sea levels: Helping decision-makers confront the inevitable. *Coastal Management*, *47*(2), 127–150. https://doi.org/10.1080/08920753.2019.1551012

Hinkel, J., J. A. Church, J. M. Gregory, E. Lambert, G. Le Cozannet, J. Lowe, et al. (2019). Meeting user needs for sea level rise information: A decision analysis perspective. *Earth's Future*, *7*(3), 320–337. https://doi.org/10.1029/2018ef001071

Hock, R., Bliss, A., Marzeion, B. E. N., Giesen, R. H., Hirabayashi, Y., Huss, M., et al. (2019). Glaciermip—A model intercomparison of global-scale glacier mass-balance models and projections. *Journal of Glaciology*, *65*(251), 453–467. https://doi.org/10.1017/jog.2019.22

Jackson, L. P., & Jevrejeva, S. (2016). A probabilistic approach to 21st century regional sea-level projections using rcp and high-end scenarios. *Global and Planetary Change*, *146*, 179–189. https://doi.org/10.1016/j.gloplacha.2016.10.006

Jevrejeva, S., Frederikse, T., Kopp, R. E., Le Cozannet, G., Jackson, L. P., & van de Wal, R. S. W. (2019). Probabilistic sea level projections at the coast by 2100. *Surveys in Geophysics*, *40*(6), 1673–1696. https://doi.org/10.1007/s10712-019-09550-y

Jevrejeva, S., Jackson, L. P., Riva, R. E., Grinsted, A., & Moore, J. C. (2016). Coastal sea level rise with warming above 2 degrees C. *Proceedings of the National Academy of Sciences of the United States of America*, *113.47*, 13342–13347. https://doi.org/10.1073/pnas.1605312113

Kopp, R. E., Horton, R. M., Little, C. M., Mitrovica, J. X., Oppenheimer, M., Rasmussen, D. J., et al. (2014). Probabilistic 21st and 22nd century sea-level projections at a global network of tide-gauge sites. *Earth's Future*, *2*(8), 383–406. https://doi.org/10.1002/2014ef000239

Le Bars, D. (2018). Uncertainty in sea level rise projections due to the dependence between contributors. *Earth's Future*, *6*(9), 12751291. https://doi.org/10.1029/2018ef000849

Levermann, A., Winkelmann, R., Albrecht, T., Goelzer, H., Golledge, N. R., Greve, R., et al. (2020). Projecting Antarctica's contribution to future sea level rise from basal ice shelf melt using linear response functions of 16 ice sheet models (larmip-2). *Earth System Dynamics*, *11.1*, 35–76. https://doi.org/10.5194/esd-11-35-2020

Little, C. M., Horton, R. M., Kopp, R. E., Oppenheimer, M., & Yip, S. (2015). Uncertainty in twenty-first-century cmip5 sea level projections. *Journal of Climate*, *28*(2), 838–852. https://doi.org/10.1175/jcli-d-14-00453.1

Marzeion, B., Hock, R., Anderson, B., Bliss, A., Champollion, N., Fujita, K., et al. (2020). Partitioning the uncertainty of ensemble projections of global glacier mass change. *Earth's Future*, *8*(7), 2328–4277. https://doi.org/10.1029/2019ef001470

Marzeion, B., Jarosch, A. H., & Hofer, M. (2012). Past and future sea-level change from the surface mass balance of glaciers. *The Cryosphere*, *6*(6), 1295–1322. https://doi.org/10.5194/tc-6-1295-2012

Melet, A., & Meyssignac, B. (2015). Explaining the spread in global mean thermosteric sea level rise in cmip5 climate models. *Journal of Climate*, *28*(24), 9918–9940. https://doi.org/10.1175/jcli-d-15-0200.1

Milne, G. A., & Mitrovica, J. X. (1998). Postglacial sea-level change on a rotating earth. *Geophysical Journal International*, *133*(1), 1–19. https://doi.org/10.1046/j.1365-246X.1998.1331455.x

Mitrovica, J. X., Tamisiea, M. E., Davis, J. L., & Milne, G. A. (2001). Recent mass balance of polar ice sheets inferred from patterns of global sea-level change. *Nature*, *409*(6823), 1026–1029. https://doi.org/10.1038/35059054

Oppenheimer, M., B. Glavovic, J. Hinkel, R. S. W. van de Wal, A. K. Magnan, A. Abd-Elgawad, et al. (2019). Sea level rise and implications for low-lying islands, coasts and communities. In H.-O. Pörtner, D. Roberts, V. Masson-Delmotte, P. Zhai, M. Tignor, E. Poloczanska, et al. (Eds.), *IPCC special report on the ocean and cryosphere in a changing climate*.

Palmer, M. D., Gregory, J. M., Bagge, M., Calvert, D., Hagedoorn, J. M., Howard, T., et al. (2020). Exploring the drivers of global and local sea-level change over the 21st century and beyond. *Earth's Future*, *8*(9), 2328–4277. https://doi.org/10.1029/2019ef001413

RGI Consortium (2017). *Randolph glacier inventory – A Dataset of Global Glacier Outlines: Verson 6.0. Report, Global Land Ice Measurements from Space*. Colorado, USA: Digital Media. https://doi.org/10.7265/N5-RGI-60

Seroussi, H., Nowicki, S., Payne, A. J., Goelzer, H., Lipscomb, W. H., Abe-Ouchi, A., et al. (2020). Ismip6 Antarctica: A multi-model ensemble of the Antarctic ice sheet evolution over the 21st century. *The Cryosphere*, *14*(9), 3033–3070. https://doi.org/10.5194/tc-14-3033-2020

Slangen, A. B. A., Carson, M., Katsman, C. A., van de Wal, R. S. W., Köhl, A., Vermeersen, L. L. A., & Stammer, D. (2014). Projecting twenty-first century regional sea-level changes. *Climatic Change*, *124*(1–2), 317–332. https://doi.org/10.1007/s10584-014-1080-9

Slater, D. A., Felikson, D., Straneo, F., Goelzer, H., Little, C. M., Morlighem, M., et al. (2020). Twenty-first century ocean forcing of the Greenland ice sheet for modelling of sea level contribution. *The Cryosphere*, *14*(3), 985–1008. https://doi.org/10.5194/tc-14-985-2020

Tamisiea, M. E., Hill, E. M., Ponte, R. M., Davis, J. L., Velicogna, I., & Vinogradova, N. T. (2010). Impact of self-attraction and loading on the annual cycle in sea level. *Journal of Geophysical Research*, *115*(C7), C07004. https://doi.org/10.1029/2009jc005687

van Vuuren, D. P., Edmonds, J., Kainuma, M., Riahi, K., Thomson, A., Hibbard, K., et al. (2011). The representative concentration pathways: An overview. *Climatic Change*, *109*(1–2), 5–31. https://doi.org/10.1007/s10584-011-0148-z

Wada, Y., Flörke, M., Hanasaki, N., Eisner, S., Fischer, G., Tramberend, S., et al. (2016). Modeling global water use for the 21st century: The water futures and solutions (wfas) initiative and its approaches. *Geoscientific Model Development*, *9*(1), 175–222. https://doi.org/10.5194/gmd-9-175-2016

Wal, R. S, van de, W., Zhang, X., Minobe, S., Jevrejeva, S., Riva, R. E. M., et al. (2019). Uncertainties in long-term twenty-first century process-based coastal sea-level projections. *Surveys in Geophysics*, *40*(6), 1655–1671. https://doi.org/10.1007/s10712-019-09575-3